

High order Chin actions in path integral Monte Carlo

K. Sakkos, J. Casulleras, and J. Boronat

*Departament de Física i Enginyeria Nuclear,
Universitat Politècnica de Catalunya,
Campus Nord B4–B5, E-08034 Barcelona, Spain*
(Dated: October 29, 2018)

Abstract

High order actions proposed by Chin have been used for the first time in path integral Monte Carlo simulations. Contrarily to the Takahashi-Imada action, which is accurate to fourth order only for the trace, the Chin action is fully fourth order, with the additional advantage that the leading fourth and sixth order error coefficients are finely tunable. By optimizing two free parameters entering in the new action we show that the time step error dependence achieved is best fitted with a sixth order law. The computational effort per bead is increased but the total number of beads is greatly reduced, and the efficiency improvement with respect to the primitive approximation is approximately a factor of ten. The Chin action is tested in a one-dimensional harmonic oscillator, a H_2 drop, and bulk liquid ^4He . In all cases a sixth-order law is obtained with values of the number of beads that compare well with the pair action approximation in the stringent test of superfluid ^4He .

PACS numbers: 31.15.Kb, 02.70.Ss

I. INTRODUCTION

Path integral Monte Carlo (PIMC) methods provide a fundamental approach in the study of interacting quantum many-body systems at low temperatures.^{1,2,3} This accurate simulation tool relies on the well-known convolution property of the thermal density matrix which allows for estimating the density matrix at low temperature from their knowledge at higher temperature, where the system is well described by classical statistical mechanics.^{4,5,6} The partition function Z of the quantum system is then written as a multidimensional integral with a distribution law that resembles the one of a closed classical polymer with an inter-bead harmonic coupling. If one either ignores the quantum statistics of the particles (*boltzmanons*), or they are bosons, then the statistical distribution law is positive definite and can be interpreted as a probability distribution function which can be sampled by standard Metropolis Monte Carlo methods. The mapping of this finite-temperature quantum system to a classic system of polymers was already suggested by Feynman⁵ and implemented in practice by Barker,⁷ and Chandler and Wolynes⁸ in their pioneering works.

In the simplest and most common implementations of the PIMC method the density matrix at high temperature, which constitutes the building block of the polymer chain, is considered fully classical, i.e., kinetic and potential parts of the action are splitted ignoring any contribution arising from the non-commutativity of the kinetic \hat{K} and potential \hat{V} operators. This approximation is known as primitive action (PA) and is accurate to order $(\beta/M)^2$, with β the inverse temperature and M the number of convolution terms (beads). When the temperature decreases the number of beads to reach convergence in terms of $1/M$ increases and the system becomes more and more quantum. In the classical limit, PIMC reduces to classic MC since the polymeric chain reduces to a single point ($M = 1$). On the other hand, near the zero-temperature limit the chains acquire extensions comparable to the size of the simulation box. PA is accurate to study semiclassical systems in which the quantum effects are comparatively small and therefore the number of beads in the asymptotic regime is low enough for an efficient sampling. However, if the interest lies in a fully quantum regime at very cold temperatures, M increases very fast making simulations hard, if not impossible, due to very low efficiency in the sampling of the long chains involved.

The study of fully quantum fluids and solids require better actions than the PA. An accurate action to deal with very low temperatures, down to superfluid regimes, relies on the pair-product approximation⁹ in which the basic piece of the PIMC chain is the exact action for two isolated particles. The pair-product action has been used extensively in the study of superfluids and it is specially accurate for hard-spherelike systems such as liquid ^4He .³ However, its use for non-radial interactions is much more difficult due to the complexity of the pair density matrix. A different approach to improve the PA relies on the use of higher-order actions obtained directly from the exponential of the Hamiltonian, $\exp(-\beta\hat{H})$. Working in this direction, Takahashi and Imada¹⁰ and later on, and independently, Li and Broughton¹¹ managed to write a new action (TIA) which is accurate to fourth order $(\beta/M)^4$ for the trace. To this end, they incorporated in the expression for the action the double commutator $[[\hat{V}, \hat{K}], \hat{V}]$. More recently, Jang *et al.*¹² proposed a new action based on the Suzuki factorization¹³ and accurate to fourth order. In spite of being a real fourth order action, and therefore better than the TIA, the results obtained by Jang *et al.*¹² do not show a significant improvement towards the reduction of the number of beads in the asymptote $\beta/M \rightarrow 0$ respect to the TIA.

In the present work, we introduce a new family of high order actions based on the sym-

plectic developments of Chin¹⁴ and Chin and Chen¹⁵ that have already proved its efficiency in solving the Schrödinger equation,¹⁶ problems in classical mechanics,¹⁷ and in the implementation of evolution operators in density functional theory.¹⁸ In Chin's factorization of the evolution operator all the coefficients are *i*) positive (and therefore directly implementable in Monte Carlo simulations) and *ii*) continuously tunable, which makes possible to force the error terms of fourth order to roughly cancel each other for the specific range of time-step values of interest for the actual simulations. We have introduced this new action in our PIMC algorithm and all the results presented in this article show that the accuracy achieved in terms of β/M is sixth order in practice in spite of the fact that the action is only accurate to fourth order. The attained reduction in the number of beads makes this algorithm competitive with the pair-product approximation in the study of quantum fluids and solids at ultralow temperatures.

The rest of the work is organized as follows. The action and the method used for the PIMC simulation is contained in Sec. II. In Sec. III, we present results obtained with the Chin's action for the one-dimensional harmonic oscillator, a drop of H₂ molecules, and bulk liquid ⁴He at low temperatures. Finally, a brief summary and the main conclusions are reported in Sec. IV.

II. FORMALISM

At finite temperature, the knowledge of the quantum partition function

$$Z = \text{Tr } e^{-\beta \hat{H}} \quad (1)$$

allows for a full microscopic description of the properties of a given system, with $\beta = 1/T$ and $\hat{H} = \hat{K} + \hat{V}$ the Hamiltonian. In a N -particle system, the kinetic operator is given by

$$\hat{K} = -\frac{\hbar^2}{2m} \sum_{i=1}^N \nabla_i^2, \quad (2)$$

and the potential one, assuming pairwise interactions, by

$$\hat{V} = \sum_{i<j}^N V(r_{ij}). \quad (3)$$

The non-commutativity of the quantum operators \hat{K} and \hat{V} makes impractical a direct calculation of the partition function Z (1). Instead, all practical implementations intended for Monte Carlo estimations of Z rely on its convolution approximation

$$e^{-\beta(\hat{K}+\hat{V})} = \left(e^{-\varepsilon(\hat{K}+\hat{V})} \right)^M, \quad (4)$$

with $\varepsilon = \beta/M$, where each one of the terms in the r.h.s. corresponds to a higher temperature MT . In the most simple approximation, known as primitive action (PA), the kinetic and potential contributions factorize

$$e^{-\varepsilon(\hat{K}+\hat{V})} \simeq e^{-\varepsilon \hat{K}} e^{-\varepsilon \hat{V}}, \quad (5)$$

the convergence to the exact result being warranted by the Trotter formula¹⁹

$$e^{-\beta(\hat{K}+\hat{V})} = \lim_{M \rightarrow \infty} \left(e^{-\varepsilon \hat{K}} e^{-\varepsilon \hat{V}} \right)^M . \quad (6)$$

The primitive action is a particular case of a more general form in which one can decompose the action, that is

$$e^{-\varepsilon(\hat{K}+\hat{V})} \simeq \prod_{i=1}^n e^{-t_i \varepsilon \hat{K}} e^{-v_i \varepsilon \hat{V}} , \quad (7)$$

with $\{t_i, v_i\}$ parameters to be determined according to the required accuracy of the approximation. As we are interested in the Monte Carlo implementation of Eq. (7), all these parameters must be positive. However, the Sheng-Suzuki^{20,21} theorem proves that this is impossible beyond second order in ε . Recently, Chin¹⁴ has analyzed these expansions (7) for the estimation of the quantum partition function where only the trace is required (1). As the trace is invariant under a similarity transformation S , it could be possible to improve the order of the approximation by a proper choice of S . However, Chin¹⁴ has proved that expansions like (7) can not be corrected with S beyond second order, generalizing in this form the Sheng-Suzuki theorem.^{20,21}

In order to overcome the limitation imposed by the Sheng-Suzuki^{20,21} theorem it is necessary to include in the operator expansion terms with double commutators such as $[[\hat{V}, \hat{K}], \hat{V}]$. In a recent work, Chin¹⁴ has proved that a second-order algorithm (PA) can be corrected by a similarity transformation if that commutator is introduced. The result yields the TIA, with a trace that is accurate to fourth order. The TIA improves significantly the accuracy of the PA in PIMC simulations but not enough to deal properly with fully quantum fluids. In order to make a step further it is necessary to work directly with real fourth-order actions. Chin and Chen¹⁵ have worked out a continuous family of gradient symplectic algorithms which are accurate to fourth order and that have proved to be extremely accurate in the resolution of classical and quantum problems. Now, we extend the focus of its applicability to the PIMC algorithm.

The fourth-order action we have used is a two-parameter model given explicitly by¹⁵

$$e^{-\varepsilon \hat{H}} \simeq e^{-v_1 \varepsilon \hat{W}_{a_1}} e^{-t_1 \varepsilon \hat{K}} e^{-v_2 \varepsilon \hat{W}_{1-2a_1}} e^{-t_1 \varepsilon \hat{K}} e^{-v_1 \varepsilon \hat{W}_{a_1}} e^{-2t_0 \varepsilon \hat{K}} , \quad (8)$$

hereafter referred as Chin action (CA). The generalized potentials \hat{W} resemble the one that appears in the TIA since both incorporate the double commutator

$$[[\hat{V}, \hat{K}], \hat{V}] = \frac{\hbar^2}{m} \sum_{i=1}^N |\mathbf{F}_i|^2 , \quad (9)$$

with \mathbf{F}_i the *force* acting on particle i ,

$$\mathbf{F}_i = \sum_{j \neq i}^N \nabla_i V(r_{ij}) . \quad (10)$$

The potentials \hat{W} in Eq. (8) are explicitly

$$\hat{W}_{a_1} = \hat{V} + \frac{u_0}{v_1} a_1 \varepsilon^2 \left(\frac{\hbar^2}{m} \sum_{i=1}^N |\mathbf{F}_i|^2 \right) \quad (11)$$

$$\hat{W}_{1-2a_1} = \hat{V} + \frac{u_0}{v_2} (1 - 2a_1) \varepsilon^2 \left(\frac{\hbar^2}{m} \sum_{i=1}^N |\mathbf{F}_i|^2 \right) . \quad (12)$$

The parameters in Eqs. (8) and (11,12) are not all independent and can be written as a function of only two, a_1 and t_0 , which are restricted to fulfill the conditions

$$0 \leq a_1 \leq 1 \quad (13)$$

$$0 \leq t_0 \leq \frac{1}{2} \left(1 - \frac{1}{\sqrt{3}} \right) . \quad (14)$$

The rest of parameters are obtained from the two independent ones $\{a_1, t_0\}$ according to the equations

$$u_0 = \frac{1}{12} \left[1 - \frac{1}{1-2t_0} + \frac{1}{6(1-2t_0)^3} \right] \quad (15)$$

$$v_1 = \frac{1}{6(1-2t_0)^2} \quad (16)$$

$$v_2 = 1 - 2v_1 \quad (17)$$

$$t_1 = \frac{1}{2} - t_0 . \quad (18)$$

The accuracy of the CA depends on the particular values of a_1 and t_0 that have to be numerically optimized. Each one modifies the action in different directions: t_0 controls the weight of the different parts in which the kinetic part is splitted (8) and a_1 the weight of each part in which the double commutator is divided (12).

Restricting first our analysis to distinguishable particles, the quantum partition function Z (1) can be obtained through a multidimensional integral of the M terms (beads) in which it is decomposed,

$$Z = \int d\mathbf{R}_1 \dots d\mathbf{R}_M \prod_{\alpha=1}^M \rho(\mathbf{R}_\alpha, \mathbf{R}_{\alpha+1}) , \quad (19)$$

with $\mathbf{R} \equiv \{\mathbf{r}_1, \dots, \mathbf{r}_N\}$ and $\mathbf{R}_{M+1} = \mathbf{R}_1$. In the rest of the work, Latin and Greek indexes are used for particles and beads, respectively. The density matrix of each step in Eq (19) is written in the CA,

$$\begin{aligned} \rho(\mathbf{R}_\alpha, \mathbf{R}_{\alpha+1}) = & \left(\frac{m}{2\pi\hbar^2\varepsilon} \right)^{9N/2} \left(\frac{1}{2t_1^2 t_0} \right)^{3N/2} \int d\mathbf{R}_{\alpha A} d\mathbf{R}_{\alpha B} \exp \left\{ -\frac{m}{2\hbar^2\varepsilon} \right. \\ & \times \sum_{i=1}^N \left(\frac{1}{t_1} (\mathbf{r}_{\alpha,i} - \mathbf{r}_{\alpha A,i})^2 + \frac{1}{t_1} (\mathbf{r}_{\alpha A,i} - \mathbf{r}_{\alpha B,i})^2 + \frac{1}{2t_0} (\mathbf{r}_{\alpha B,i} - \mathbf{r}_{\alpha+1,i})^2 \right) \\ & - \varepsilon \sum_{i < j}^N (v_1 V(r_{\alpha,ij}) + v_2 V(r_{\alpha A,ij}) + v_1 V(r_{\alpha B,ij})) \\ & \left. - \varepsilon^3 u_0 \frac{\hbar^2}{m} \sum_{i=1}^N (a_1 |\mathbf{F}_{\alpha,i}|^2 + (1-2a_1) |\mathbf{F}_{\alpha A,i}|^2 + a_1 |\mathbf{F}_{\alpha B,i}|^2) \right\} . \end{aligned} \quad (20)$$

According to the CA, each elementary block of *width* ε is splitted into three, with two middle points that we have denoted as A and B in the above expression for the density matrix (20). Each one of the three internal beads resembles a bead in the TIA approximation in the sense

that the beads of the same type $\{\alpha, \alpha A, \alpha B\}$ interact through a generalized Takahashi-Imada potential, but with different weights in front of the double-commutator term (11,12). The estimators for the total and partial energies of the system are therefore similar to the ones derived in the TIA approximation.

The total and kinetic energy per particle can be readily derived from first derivatives of the quantum partition function Z ,

$$\frac{E}{N} = -\frac{1}{NZ} \frac{\partial Z}{\partial \beta} \quad (21)$$

$$\frac{K}{N} = \frac{m}{N\beta Z} \frac{\partial Z}{\partial m}, \quad (22)$$

the potential energy being the difference $V/N = E/N - K/N$. The potential energy can also be derived through the relation¹⁰

$$O(\mathbf{R}) = -\frac{1}{\beta} \frac{1}{Z(V)} \left. \frac{dZ(V + \lambda O)}{d\lambda} \right|_{\lambda=0}, \quad (23)$$

that can be used also for the estimation of other coordinate operators. From the definition (22), which is known as thermodynamic estimator, the kinetic energy per particle results in

$$\frac{K^{th}}{N} = \frac{9}{2\varepsilon} - \frac{1}{MN} \left(\frac{m}{2\hbar^2 \varepsilon^2} T_{MN}^t - \frac{\hbar^2}{m} \varepsilon^2 u_0 W_{MN} \right), \quad (24)$$

with

$$T_{MN}^t = \sum_{\alpha=1}^M \sum_{i=1}^N \left[\frac{1}{t_1} (\mathbf{r}_{\alpha,i} - \mathbf{r}_{\alpha A,i})^2 + \frac{1}{t_1} (\mathbf{r}_{\alpha A,i} - \mathbf{r}_{\alpha B,i})^2 + \frac{1}{2t_0} (\mathbf{r}_{\alpha B,i} - \mathbf{r}_{\alpha+1,i})^2 \right], \quad (25)$$

and

$$W_{MN} = \sum_{\alpha=1}^M \sum_{i=1}^N [a_1 |\mathbf{F}_{\alpha,i}|^2 + (1 - 2a_1) |\mathbf{F}_{\alpha A,i}|^2 + a_1 |\mathbf{F}_{\alpha B,i}|^2], \quad (26)$$

The potential energy can be calculated from the difference between the total energy and the kinetic one (24) or by means of the general relation (23) with identical result,

$$\frac{V}{N} = \frac{1}{MN} \left(V_{MN} + 2 \frac{\hbar^2}{m} \varepsilon^2 u_0 W_{MN} \right), \quad (27)$$

with

$$V_{MN} = \sum_{\alpha=1}^M \sum_{i < j}^N [v_1 V(r_{\alpha,ij}) + v_2 V(r_{\alpha A,ij}) + v_1 V(r_{\alpha B,ij})], \quad (28)$$

and W_{MN} given by Eq. (26). This term that appears both in the total and kinetic energy, but with different weight, comes from the derivative with respect to β and with respect to m , respectively, of the W potentials (11,12), which depend explicite on the temperature and the mass.

The variance of the thermodynamic estimation of the kinetic energy (24) can be rather large and increases with the number of beads M .^{22,23} This well-known problem is generally

solved by using the virial estimator²² of the kinetic energy which relies on the invariance of the partition function under a scaling of the coordinate variables $\mathbf{r} \rightarrow \lambda \mathbf{r}$. The centroid version of the virial estimator for the CA is given by

$$\frac{K^{\text{cv}}}{N} = \frac{3}{2\beta} + \frac{1}{MN} \left(\frac{1}{2} T_{MN}^{\text{v}} + \frac{\hbar^2}{m} \varepsilon^2 u_0 (W_{MN} + Y_{MN}) \right). \quad (29)$$

In this expression, W_{MN} is given by Eq. (26) and the two other terms are explicitly

$$T_{MN}^{\text{v}} = \sum_{\alpha=1}^M \sum_{i=1}^N [v_1(\mathbf{r}_{\alpha,i} - \mathbf{r}_{o,i}) \mathbf{F}_{\alpha,i} + v_2(\mathbf{r}_{\alpha A,i} - \mathbf{r}_{o,i}) \mathbf{F}_{\alpha A,i} + v_1(\mathbf{r}_{\alpha B,i} - \mathbf{r}_{o,i}) \mathbf{F}_{\alpha B,i}] \quad (30)$$

and

$$\begin{aligned} Y_{MN} = & \sum_{\alpha=1}^M \sum_{i=1}^N \sum_{j \neq i}^N [a_1(r_{\alpha,i} - r_{o,i})^a T(\alpha, i, j)_a^b (F_{\alpha,i} - F_{\alpha,j})_b \\ & + (1 - 2a_1)(r_{\alpha A,i} - r_{o,i})^a T(\alpha A, i, j)_a^b (F_{\alpha A,i} - F_{\alpha A,j})_b \\ & + a_1(r_{\alpha B,i} - r_{o,i})^a T(\alpha B, i, j)_a^b (F_{\alpha B,i} - F_{\alpha B,j})_b] . \end{aligned} \quad (31)$$

In the above expressions, $\mathbf{r}_{o,i}$ is the center of mass (centroid) of the chain representing the atom i . The indexes a, b in the definition of Y_{MN} (31) stand for the Cartesian coordinates and an implicit summation over repeated indices is assumed. The tensor T appears also in the virial estimation of the kinetic energy in the TIA approximation and is explicitly given by²⁴

$$\begin{aligned} T(\gamma, i, j)_a^b = & \left[\frac{\delta_a^b}{r_{\gamma,ij}} - \frac{(r_{\gamma,ij})^b (r_{\gamma,ij})_a}{r_{\gamma,ij}^3} \right] \frac{dV(r_{\gamma,ij})}{dr_{\gamma,ij}} \\ & + \frac{(r_{\gamma,ij})^b (r_{\gamma,ij})_a}{r_{\gamma,ij}^2} \frac{d^2 V(r_{\gamma,ij})}{dr_{\gamma,ij}^2}, \end{aligned} \quad (32)$$

where γ stands for the three different types of internal beads, α , αA , and αB , and $\delta_a^b = 1$ if $a = b$ and 0 otherwise.

The implementation of the CA in the PIMC algorithm is similar to the one for the TIA. Going from TIA to CA, one has to split a single bead into three (with different link lengths), but in these new beads the different atoms interact with a similar generalized potential, coming from the double commutator. A simple inspection on the equations of the density matrix and energies for the CA and TIA shows that the complexity of both actions are essentially the same and require, for example, the same order of derivatives of the interatomic potential $V(r)$.

A final concern that any PIMC calculation must afford is whether the sampling method has the necessary efficiency in the movement of the chains to avoid the slowing down that can appear for long chains when using only individual bead movements. In this sense, the implementation in the algorithm of collective smart movements is crucial. To this end, we use the staging method^{9,25,26} combined with movements of the center of mass of each one of the atoms. In the CA, the length of each chain is not the same and therefore one has to generalize the staging method. This generalization is discussed in Appendix A.

III. RESULTS

We have studied the accuracy of the high-order action proposed by Chin in three different systems: a one-dimensional harmonic oscillator, a drop of H_2 molecules, and bulk liquid ^4He . The harmonic oscillator is a very simple system but it has the advantage of its exact analytic solution at any temperature which allows for an accurate test of the method. The H_2 drop is a more exigent test and it has been adopted in previous works as benchmark for testing different actions. Finally, liquid ^4He is also a well-known system with a wide experimental information available for comparison and with the appealing feature of remaining liquid even at zero temperature. In all the simulations we have used a sampling method which combines movements of the center of mass of the chains and smart movements of chain pieces with the staging technique.^{9,25,26} The length of the staging chain and the maximum value of the displacement of the center of mass are chosen to achieve an acceptance rate of 30%-50%. The results presented below have been checked to be stable with respect to the frequency and size of both movements.

A. Harmonic oscillator

In our first application, we consider a particle in a one-dimensional harmonic oscillator with Hamiltonian

$$H = -\frac{\hbar^2}{2m} \frac{\partial^2}{\partial x^2} + \frac{1}{2} m \omega^2 x^2 . \quad (33)$$

As it is well known, this problem can be exactly solved at any temperature and, in particular, the energy is given by⁶

$$E = \frac{1}{2} \hbar \omega \coth(\beta \hbar \omega / 2) . \quad (34)$$

In the PIMC simulations we have taken $\omega = \hbar = m = 1$ and the results presented correspond to temperatures $T = 0.1$ and 0.2 . The energies obtained at $T = 0.2$ with different actions and as a function of the number of beads M are contained in Table I, and have to be compared with the exact value 0.50678 . In order to reproduce the exact energy with these five digits PA requires the use of $M = 512$ and TIA of a quite smaller number $M = 32$.²⁴ This asymptotic value is reached in the CA case with a sizeable smaller number: $M = 6$ and $M = 5$ for $a_1 = 0$ and $a_1 = 0.33$, respectively.

In Fig. 1, the energies for the different actions at $T = 0.2$ are plotted as a function of ε . The lines on top of the PIMC data correspond to polynomial fits of the form

$$E = E_0 + A_\delta \varepsilon^\delta \quad (35)$$

to the energies close to the common asymptotic value E_0 . From previous work²⁴ it is known that $\delta = 2$ and 4 for PA and TIA, respectively. In the case of the CA approximation the departure from E_0 is effectively of sixth order $\delta = 6$ in spite of the fact that CA is rigorously a fourth-order action. This result can be understood as a partial but effective cancellation between the leading errors of fourth and higher orders due to the fact that the CA (8) is written in terms of two parameters t_0 and a_1 that can be optimized within some constraints(13,14). We show in Fig. 2 the characteristic behavior of the energy as a function of ε and for different choices of t_0 and a fixed value for a_1 . The lines are fits to the PIMC data for values of t_0 in the range 0.9 - 0.15 (top to bottom for large ε values in the

M	E_{PA}	E_{TIA}	$E_{\text{CA}}(a_1 = 0)$	$E_{\text{CA}}(a_1 = 0.33)$
2	0.30755	0.44702	0.50444	0.50643
3			0.50649	0.50675
4	0.43162	0.50053	0.50673	0.50677
5			0.50677	0.50678
6			0.50678	0.50678
7			0.50678	
8	0.48424	0.50630		
16	0.50085	0.50675		
32	0.50528	0.50678		
64	0.50641	0.50678		
128	0.50669			
256	0.50676			
512	0.50678			

TABLE I: PA (E_{PA}), TIA (E_{TIA}), and CA (E_{CA}) results for the one-dimensional harmonic oscillator at $T = 0.2$.

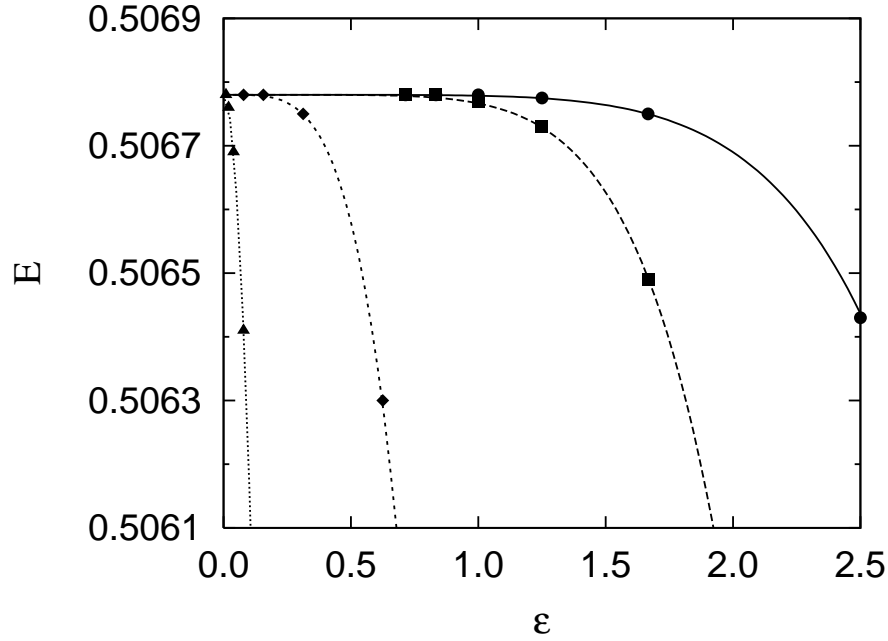


FIG. 1: PIMC energy of a particle in a one-dimensional harmonic well as a function of ε . Triangles, diamonds, squares and circles stand for PA, TIA, CA ($a_1 = 0$), and CA ($a_1 = 0.33$), respectively. The lines correspond to polynomial fits (35) to the data. The errorbars are smaller than the size of the symbols.

figure). When $t_0 < 0.13$ the asymptotic exact value is approached from above and contrarily from below when $t_0 \geq 0.13$. By adjusting in a proper way the value of t_0 it is therefore possible to achieve a nearly flat dependence with ε and consequently to improve empirically the fourth-order accuracy of the CA.

The estimation of the optimal value of the parameter t_0 for a fixed a_1 can be better made

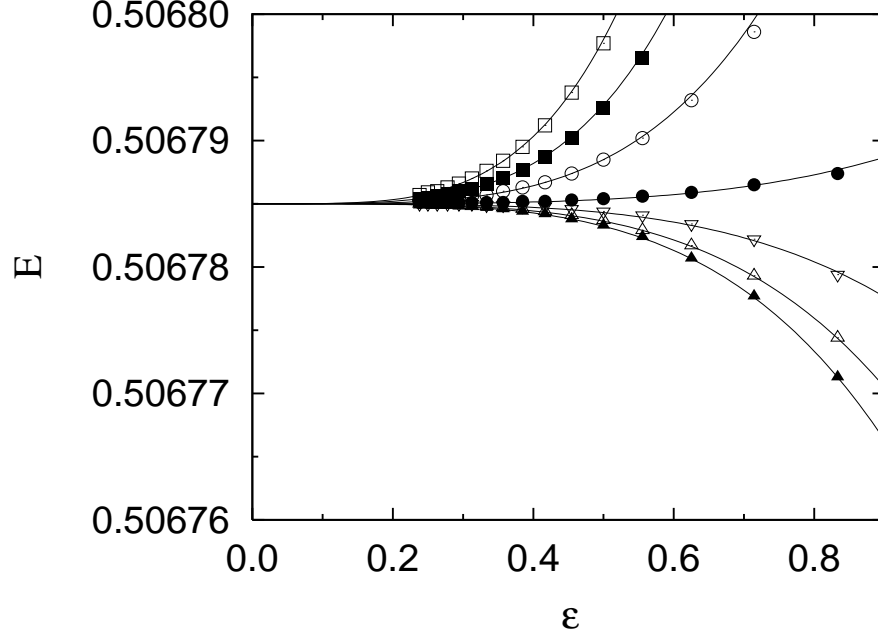


FIG. 2: Departure from the asymptotic energy E_0 for different values of t_0 and a fixed value for a_1 ($a_1 = 0.33$). From top to bottom, $t_0 = 0.09, 0.10, 0.11, 0.12, 0.13, 0.14$, and 0.15 . The temperature is $T = 0.2$.

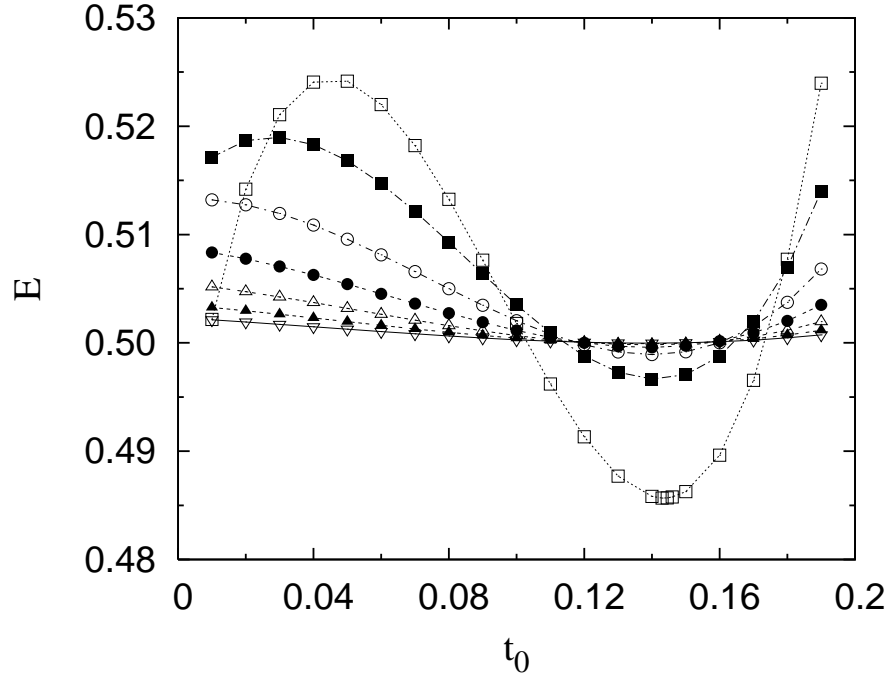


FIG. 3: Energies as a function of the parameter t_0 for $a_1 = 0.33$, and for different number of beads, at $T = 0.1$. Squares, $M = 2$; filled squares, $M = 3$; circles, $M = 4$; filled circles, $M = 5$; up triangles, $M = 6$; up filled triangles, $M = 7$; down triangles, $M = 8$.

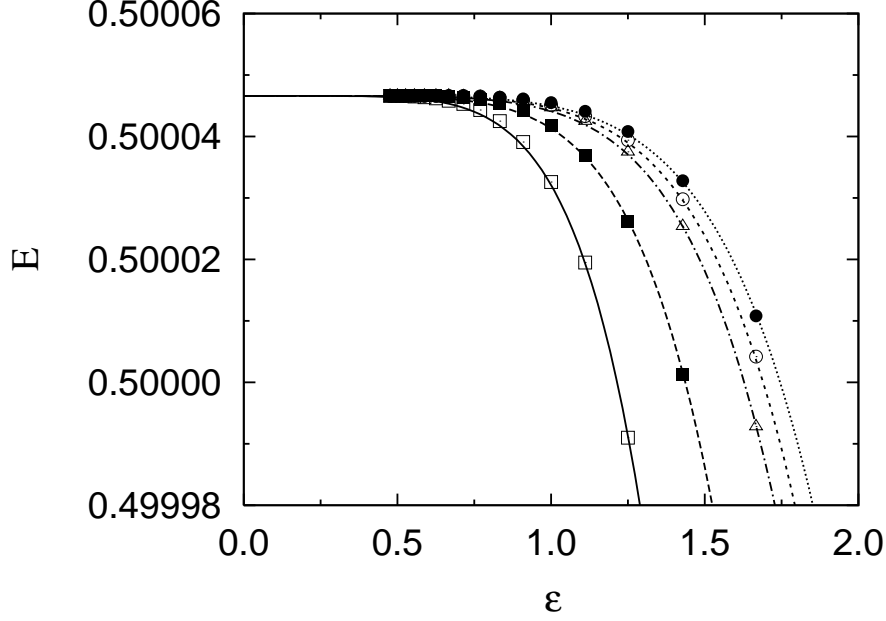


FIG. 4: Energies as a function of ε for different values of the parameter a_1 at $T = 0.1$. Squares, $a_1 = 0$; filled squares, $a_1 = 0.14$; circles, $a_1 = 0.25$; filled circles, $a_1 = 0.33$; triangles, $a_1 = 0.45$. The optimal values of t_0 are, respectively, 0.1430, 0.0724, 0.1094, 0.1215, and 0.1298. The lines are polynomial fits (35) to the PIMC data.

by computing the energies for an increasing number of beads, starting for a low value. The behavior observed, which is similar for any allowed a_1 value, it is shown in Fig. 3 for the particular case of $a_1 = 0.33$ and $T = 0.1$. The lines on top of the data are guides to the eye and each one of them correspond to a particular M in the range $M = 2-8$. As one can see, there are two small intervals in the t_0 scale where the curves tend to intersect (around 0.12 and 0.16) and therefore where the convergence to the asymptotic value is faster. By examining the energies inside these two regimes one observes that the dependence with M is slightly smoother in the first one corresponding to smaller t_0 's. Thus, we work in this first regime and normally by selecting a value in which the approach to the exact energy is from below. For example, for this value $a_1 = 0.33$ we have chosen $t_0 = 0.1215$. It is worth noticing that this optimal value does not depend on temperature and consequently it can be adjusted working at higher temperatures where the number of beads required to achieve convergence is always smaller and thus *cheaper* from a computational point of view. We have verified that the best value of t_0 , for a given a_1 , obtained through this numerical optimization agrees with the analytical relation for the harmonic oscillator obtained in Ref. 27, which predicts the optimal parameters that cancel exactly the fourth-order error terms.

The optimal t_0 depends on the particular value of a_1 and the achieved accuracy depends also slightly on a_1 . This is explicitly shown in Fig. 4 where the dependence of the energy on ε is plotted for values of a_1 ranging from 0 to 0.45. The results correspond to $T = 0.1$ and the lines correspond to fits (35) with $\delta = 6$. In all cases the accuracy is of the same order but the best performance is achieved for $a_1 = 0.33$ which, according to the expression of the CA, is the case where the generalized potential W (11,12) acts with the same weight in the three points in which a single step ε is splitted.

M	$(E/N)_{\text{PA}}$	$(E/N)_{\text{TIA}}$	$(E/N)_{\text{CA}}$
2			-40.44(5)
4			-28.77(3)
8	-45.28(3)	-31.17(3)	-21.27(2)
10			
12			-19.13(3)
14			
16	-30.59(3)	-23.48(3)	-18.32(2)
18			
20			-17.95(3)
24			-17.81(2)
28			-17.73(2)
32	-22.97(3)	-19.49(3)	-17.66(2)
36			-17.68(2)
48			-17.68(2)
64	-19.57(3)	-18.05(3)	
128	-18.28(3)	-17.78(3)	
256	-17.89(3)	-17.72(3)	
512	-17.76(3)		

TABLE II: PA, TIA, and CA results for the energy per particle of a drop composed by $N = 22$ H_2 molecules at $T = 6$ K for different values of M . All the energies are in K. The figures in parenthesis are the statistical errors affecting the last digit.

B. H_2 drop

The case study of a drop composed by a few number of hydrogen molecules has been used in the past to compare the efficiencies of different PIMC methods and, in particular, of several approximations for the action. For this purpose, this system was used for the first time by Chakravarty *et al.*²⁸ to compare the efficiency of Fourier vs. standard PIMC methods. Later on, it was studied by Predescu *et al.*²⁹ in a comparative analysis of energy estimators and by Yamamoto³⁰ in a fourth-order calculation of small atomic and molecular drops.

The drop studied is composed by $N = 22$ H_2 molecules which are considered spherical since we restrict our calculation to the $J = 0$ state, i.e., to parahydrogen. The interaction potential is of the form

$$V(\mathbf{r}_1, \dots, \mathbf{r}_N) = \sum_{i < j}^N V_2(r_{ij}) + \sum_{i=1}^N V_c(r_i) , \quad (36)$$

with V_2 the intermolecular interaction, assumed to be of Lennard-Jones type

$$V_2(r_{ij}) = 4\epsilon \left[\left(\frac{\sigma}{r_{ij}} \right)^{12} - \left(\frac{\sigma}{r_{ij}} \right)^6 \right] \quad (37)$$

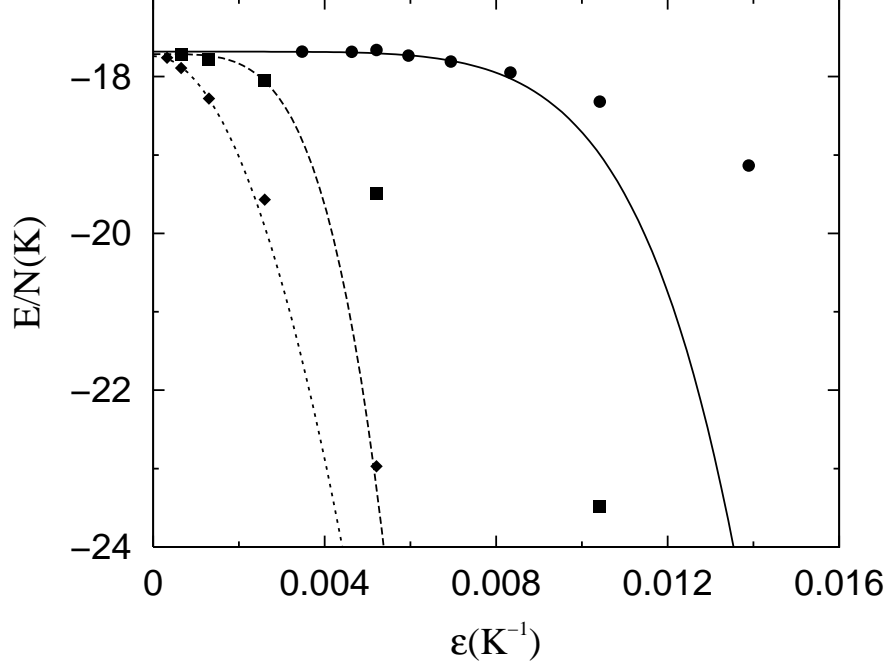


FIG. 5: Energy of the H_2 drop at $T = 6$ K as a function of ϵ for different actions: PA, diamonds; TIA, squares; circles, CA. The parameters of the CA are $a_1 = 0$ and $t_0 = 0.175$. The lines are polynomial fits (35) to the PIMC data.

and V_c is a confining potential introduced to suppress possible evaporation of molecules,

$$V_c(r_i) = \epsilon \left(\frac{|\mathbf{r}_i - \mathbf{R}_{\text{CM}}|}{R_c} \right)^{20}. \quad (38)$$

In V_c , $\mathbf{R}_{\text{CM}} = \sum_{i=1}^N \mathbf{r}_i / N$ is the position of the center of mass of the drop and R_c controls the maximum allowed distance of a particle to \mathbf{R}_{CM} . As in previous work in this problem,²⁸ we have chosen $R_c = 4\sigma$, with Lennard-Jones parameters $\sigma = 2.96$ Å and $\epsilon = 34.2$ K (37).

In Table II, we report our results for the energy of the drop using different number of beads M and several approximations for the action: PA, TIA, and CA. The asymptotic (unbiased) energy is obtained in the limit $\epsilon \rightarrow 0$ ($M \rightarrow \infty$): this is achieved with $M \simeq 512$, 128, and 32 for PA, TIA, and CA, respectively. Therefore, also in this more exigent test the CA shows its appreciably higher efficiency with respect to TIA and other published data of the same problem obtained with Suzuki actions.³⁰ The value of ϵ required to reach the asymptote in CA is comparable with the one observed in a previous study of this H_2 drop using the pair action approximation.²⁸ As it is shown in Fig. 5, the $\epsilon \rightarrow 0$ behavior is well reproduced by the polynomial fit (35) with different exponents: $\delta = 2, 4$, and 6 for PA, TIA, and CA, respectively. Our best result for the energy of the drop is obtained from the simulation with the CA: the total energy is $E/N = -17.68(2)$ K, and the potential and kinetic energies are $V/N = -47.82(3)$ K and $K/N = 30.14(2)$ K, respectively. These three energies are in agreement with the previous estimations of Refs. 28,29,30.

Going down in temperature, the PIMC calculation becomes harder due to the increase in the number of beads necessary to achieve convergence and to the simultaneous decrease of the acceptance rate in the staging movements. In order to be effectively able to compute properties in these ultracold regimes the action in use has to be accurate enough to reduce

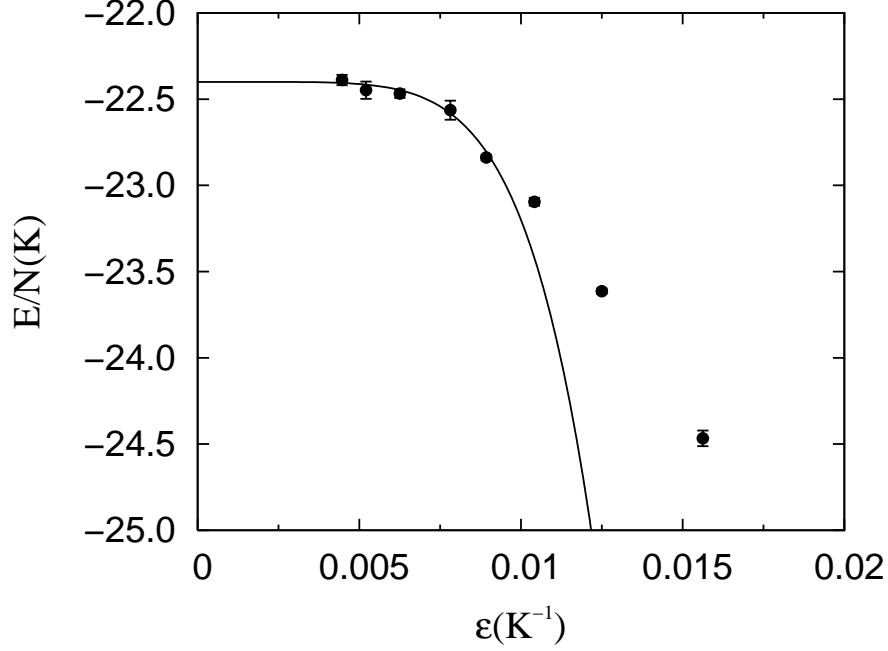


FIG. 6: Energy of the H_2 drop at $T = 1$ K as a function of ϵ using the CA. The line is a polynomial fit (35) to the PIMC data with $\delta = 6$.

M to a manageable level. To this end, we have computed the properties of the $N = 22$ drop at $T = 1$ K. In this simulation, as in the one at $T = 6$ K, we have ignored the Bose statistics of the molecules. The dependence of the total energy with ϵ is shown in Fig. 6. As one can see, the value of ϵ ($M = 180$) in the asymptote is approximately a factor of two smaller than the one at $T = 6$ K (Fig. 5) but a sixth-order behavior is again observed (solid line in Fig. 6). The energies in the asymptotic regime are $E/N = -22.47(5)$ K, $V/N = -52.7(2)$ K, and $K/N = 30.2(2)$ K. It is worth noticing that at this lower temperature PA would require the use of $M \sim 3000$ and TIA of $M \sim 1200$, values which make quite unreliable their use in the deep quantum regime.

C. Liquid ^4He

As in our previous work,²⁴ we have studied the accuracy of the CA in a fully many-body calculation, deep in the quantum regime, as it is liquid ^4He . We consider a bulk system at a density $\rho = 0.02186 \text{ \AA}^{-3}$ and at two temperatures, $T = 5.1$ and 0.8 K. The calculation is performed within a simulation box of 64 atoms with periodic boundary conditions and with an accurate Aziz potential.³¹ In order to correct for the finite size of the system we have added standard potential energy tail corrections relying on the assumption that beyond $L/2$, with L the size of the box, the medium is homogeneous, i.e. $g(r) \simeq 1$.

Table III contains PIMC results for the energy at $T = 5.1$ K using different number of beads and for several actions: PA, TIA, and CA with $a_1 = 0$ and $a_1 = 0.33$. The parameter t_0 has been optimized for both values of a_1 : $t_0 = 0.17$ and 0.082 for $a_1 = 0$ and 0.33 , respectively. As we noted in our previous study,²⁴ the introduction of the double commutator within the TIA reduces sizably the number of beads with respect to PA: the value $M = 256$ of PA turns to $M = 64$ for the TIA. The latter M is again considerably

M	$(E/N)_{\text{PA}}$	$(E/N)_{\text{TIA}}$	$(E/N)_{\text{CA}} (a_1 = 0)$	$(E/N)_{\text{CA}} (a_1 = 0.33)$
3			-5.59(3)	-5.48(3)
4			-4.51(3)	-4.40(3)
5			-3.91(3)	-3.77(3)
6			-3.53(3)	-3.43(3)
8	-9.29(3)	-6.30(3)	-3.16(3)	-3.08(3)
10			-3.01(3)	-2.89(3)
12			-2.91(3)	-2.83(3)
14			-2.86(3)	-2.81(3)
20			-2.81(3)	
16	-5.85(3)	-3.97(3)		
32	-3.98(3)	-3.04(3)		
44		-2.93(4)		
64	-3.19(4)	-2.85(4)		
100		-2.83(4)		
128	-2.92(4)	-2.82(4)		
256	-2.84(4)			
512	-2.81(4)			

TABLE III: PA, TIA, and CA ($a_1 = 0$ and $a_1 = 0.33$) results for the energy per particle of bulk liquid ^4He at $T = 5.1$ K for different values of M . All the energies are in K. The figures in parenthesis are the statistical errors affecting the last digit.

reduced by using the CA since the convergence to the exact energy is reached for a value as low as $M = 12$ ($a_1 = 0.33$). The different dependence on ε of the three models for the action is shown in Fig. 7 at $T = 5.1$ K. We can observe that the departure from the asymptote E_0 follows the same power-law dependence (35) than in the harmonic oscillator and H_2 drop previously analyzed: $\delta = 2, 4$, and 6 for PA, TIA, and CA, respectively.

The accuracy of the CA has been a bit more stressed by repeating the PIMC simulation at a lower temperature, $T = 0.8$ K. At this temperature, the quantum effects are bigger than at $T = 5.1$ K and the use of TIA, and even more PA, is completely unreliable due to the large number of beads that are necessary to eliminate the bias due to a finite M value. At 0.8 K, liquid ^4He is below the λ transition ($T_\lambda = 2.17$ K) and therefore it is superfluid making absolutely necessary the sampling of permutations to accomplish with its boson statistics. The exchange frequency is drastically reduced over T_λ and thus the inclusion of permutations at the higher temperature (5.1 K) does not modify the results presented above. Results for the energy per particle at $T = 0.8$ K as a function of ε and using the CA are shown in Fig. 8. The simulations have been carried out including or not the right symmetry of the thermal density matrix; as one can see, and is well known, the inclusion of permutations leads to a decrease of the energy which is in agreement with the experimental data on this system. The sampling of permutations is performed within the widely used method proposed by Pollock and Ceperley.^{3,9} The accuracy of the CA is the same including or not permutations in the sampling, i.e., sixth order in ε (solid lines in Fig. 8). The values of ε at which the asymptotic trend is observed are similar to the ones achieved using the pair action,³ which is the most widely used approximation to deal with superfluids within

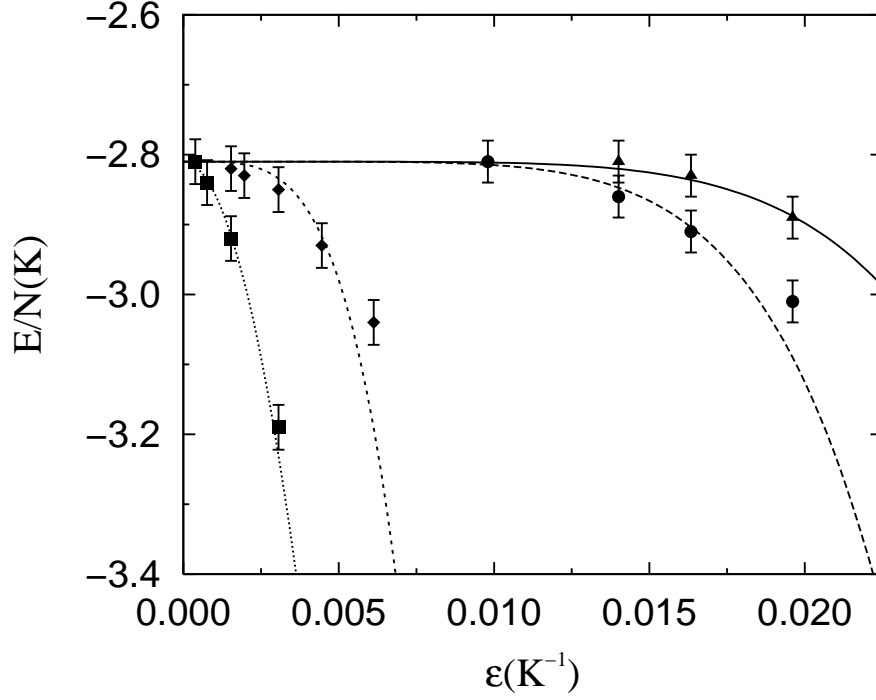


FIG. 7: Energy per particle of liquid ^4He at $T = 5.1$ K and density $\rho = 0.02186 \text{ \AA}^{-3}$ as a function of ϵ using several actions: PA, squares; TIA, diamonds; CA ($a_1 = 0$), circles; CA ($a_1 = 0.33$), triangles. The lines are polynomial fits (35) to the PIMC data with $\delta = 2, 4$, and 6 for PA, TIA, and CA, respectively.

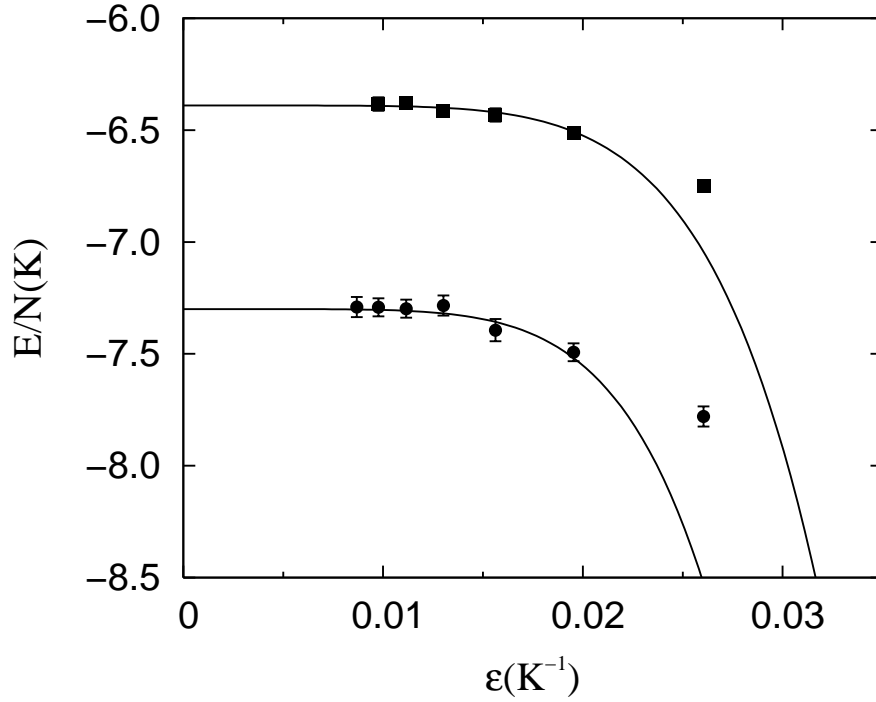


FIG. 8: Energy per particle of liquid ^4He at $T = 0.8$ K and density $\rho = 0.02186 \text{ \AA}^{-3}$ as a function of ϵ using the CA. Circles and squares correspond to a simulation including symmetrization of the density matrix or not, respectively. The lines are polynomial fits (35) with $\delta = 6$.

	CPU cost per bead	Decrease of M	Efficiency
PA	1.0	1	1.0
TIA	2.9	4	1.4
CA	7.2	58	8.0

TABLE IV: Comparison among the efficiencies of the PA, TIA, and CA in PIMC.

the PIMC formalism.

IV. CONCLUSIONS

In the last decades there has been a continued effort for improving the action to be used in PIMC simulations beyond the PA. Working directly on the exponential of the Hamiltonian, Takahashi and Imada¹⁰ introduced in the action the double commutator $[[\hat{V}, \hat{K}], \hat{V}]$ and showed that the new algorithm (TIA) was of fourth order. As showed in previous work,²⁴ the TIA reduces significantly the number of beads to reach the asymptotic limit and therefore it can be very useful in quantum systems if the temperature is not very small. However, if one is interested on achieving lower temperatures, deep in the quantum regime, the TIA is still not accurate enough since the number of beads required is yet too large. As pointed out by Chin,¹⁴ this relative failure of TIA is due to the fact that the TIA is in fact a fourth-order action but only for the trace. Posterior attempts of improving the action,^{12,30} based on actions proposed by Suzuki,¹³ did not show a significant enhancement of the efficiency of the method with respect to TIA.

Following with the aim of going a step further on the improvement of the action for PIMC applications, we have used for the first time the new developments of Chin^{14,15} that have led to full fourth-order expansions of the exponential of the Hamiltonian. The resulting action (CA) is more involved than the TIA and Suzuki action but still it is readily implementable starting on a TIA approach since the basic ingredients of the CA are already contained in the TIA. In Table IV, we compare the efficiency of the three models for the action; the numbers correspond to the calculation of liquid ^4He but are similar to the ones obtained in the study of the H_2 drop. Considering as 1 the CPU time per bead and the efficiency in the PA one observes that the cost per bead in TIA is 2.9 and the number of beads is 4 times smaller, leading to an efficiency $4/2.9 = 1.4$. In the CA, the CPU cost per bead is larger since every step ε is splitted into three but the big decrease in the number of beads (58 times smaller than in PA) results in an efficiency 8 times larger than the PA.

In the Chin action there are two parameters (t_0, a_1) that have to be optimized. The search of these parameters for a given system is not difficult since they are independent of temperature and therefore they can be found at higher temperatures where the number of beads is very small and consequently the simulations very short in CPU time. As we have discussed in the harmonic oscillator problem, the exact energy is crossed by changing t_0 because the departure from the asymptote can be upwards or downwards depending on its particular value. This behavior makes possible to search for optimal parameters that improve the efficiency of the action from fourth-order to an effective sixth order. This behavior is not only characteristic of the harmonic oscillator but completely general as we have verified in real many-body problems as the H_2 drop and bulk liquid ^4He . This sixth-order law

is maintained even at superfluid temperatures making that the number of beads required for the simulations is completely manageable. Therefore, the CA is a realistic alternative to the pair action for dealing with quantum liquids and solids in the superfluid regime at temperatures close to zero. Its implementation is not much more involved than the TIA, easier to use than the pair action, and useful also for problems with non-radial interactions where the application of pair action is much more involved. Work is also in progress to use the CA in a path integral ground state (PIGS) approach to study the limit of zero temperature, the initial simulations showing also a sixth-order accuracy and convergence to the exact energies with a few number of beads.

Acknowledgments

We wish to thank stimulating discussions with Siu Chin about high order actions. Partial financial support from DGI (Spain) Grant No. FIS2008-04403 and Generalitat de Catalunya Grant No. 2005SGR-00779 are also acknowledged.

APPENDIX: STAGING TRANSFORMATION

The staging technique allows for a direct sampling of the free (kinetic) part of the action, i.e., Metropolis test is not necessary. In this Appendix, we generalize the standard staging method to the one required for the CA action where the *width* of a given bead depend of its type ($t_1\varepsilon$, $2t_0\varepsilon$) (20). If two points of the chain representing an atom are considered fixed, \mathbf{r}_0 and \mathbf{r}_M , one is interested in transforming the free action between these two extremes

$$S \equiv \exp \left[- \sum_{\alpha=1}^M c_{\alpha} (\mathbf{r}_{\alpha} - \mathbf{r}_{\alpha-1})^2 \right] , \quad (\text{A.1})$$

into the staging one

$$S_{\text{st}} = C(\mathbf{r}_0, \mathbf{r}_M) \exp \left\{ - \sum_{\alpha=1}^{M-1} q_{\alpha} [\mathbf{r}_{\alpha} - (a_{\alpha} \mathbf{r}_{\alpha-1} + b_{\alpha} \mathbf{r}_M)]^2 \right\} . \quad (\text{A.2})$$

The constant C depends only on the fixed positions \mathbf{r}_0 and \mathbf{r}_M and therefore it is not important for the purpose of the sampling. By imposing that both actions (A.1,A.2) are equal one can derive sequential relations for the staging coefficients q_{α} , a_{α} , and b_{α} as a function of the known ones of the original action c_{α} ,

$$q_{\alpha} = c_{\alpha} + c_{\alpha+1} - q_{\alpha+1} a_{\alpha+1}^2 \quad (\text{A.3})$$

$$a_{\alpha} = c_{\alpha} / q_{\alpha} \quad (\text{A.4})$$

$$b_{\alpha} = (q_{\alpha+1} a_{\alpha+1} b_{\alpha+1} + c_M \delta_{\alpha, M-1}) / q_{\alpha} , \quad (\text{A.5})$$

with $\delta_{\alpha, M-1} = 1$ if $\alpha = M-1$ and 0 otherwise. These relations have to be applied recursively from $M-1$ to 1 with the starting conditions $q_M = a_M = b_M = 0$.

Once all the staging coefficients are determined through Eqs A.3-A.5, the new positions \mathbf{r}_α are recursively obtained from 1 to $M - 1$ using Gaussian displacements.

-
- ¹ M. J. Gillan, in *Computer Modelling of Fluids, Polymers and Solids*, edited by C. R. A. Catlow *et al.* (Kluwer, Dordrecht, 1990).
 - ² C. Chakravarty, *Int. Rev. Phys. Chem.* **16**, 421 (1997).
 - ³ D. M. Ceperley, *Rev. Mod. Phys.* **67**, 279 (1995).
 - ⁴ R. P. Feynman and A. R. Hibbs, *Quantum Mechanics and Path Integrals* (McGraw-Hill, New York, 1965).
 - ⁵ R. P. Feynman, *Statistical Mechanics* (Benjamin, New York, 1972).
 - ⁶ H. Kleinert, *Path Integrals in Quantum Mechanics, Statistics, and Polymer Physics* (World Scientific, Singapore, 1995).
 - ⁷ J. Barker, *J. Chem. Phys.* **70**, 2914 (1979).
 - ⁸ D. Chandler and P. G. Wolynes, *J. Chem. Phys.* **74**, 4078 (1981).
 - ⁹ E. L. Pollock and D. M. Ceperley, *Phys. Rev. B* **30**, 2555 (1984).
 - ¹⁰ M. Takahashi and M. Imada, *J. Phys. Soc. Jpn.* **53**, 3765 (1984).
 - ¹¹ X. P. Li and J. Q. Broughton, *J. Chem. Phys.* **86**, 5094 (1987).
 - ¹² S. Jang, S. Jang, and G. A. Voth, *J. Chem. Phys.* **115**, 7832 (2001).
 - ¹³ M. Suzuki, *Phys. Lett. A* **201**, 425 (1995).
 - ¹⁴ S. A. Chin, *Phys. Rev. E* **69**, 046118 (2004).
 - ¹⁵ S. A. Chin and C. R. Chen, *J. Chem. Phys.* **117**, 1409 (2002).
 - ¹⁶ S. A. Chin, *Phys. Rev. E* **76**, 056708 (2007).
 - ¹⁷ S. A. Chin, *Phys. Rev. E* **77**, 066401 (2008).
 - ¹⁸ E. R. Hernández, S. Janecek, M. Kaczmariski, and E. Krotscheck, *Phys. Rev. B* **75**, 075108 (2007).
 - ¹⁹ H. F. Trotter, *Proc. Am. Math. Soc.* **10**, 545 (1959).
 - ²⁰ Q. Sheng, *IMA J. Num. Analysis* **9**, 199 (1989).
 - ²¹ M. Suzuki, *J. Math. Phys.* **32**, 400 (1991).
 - ²² M. F. Herman, E. J. Bruskin, and B. J. Berne, *J. Chem. Phys.* **76**, 5150 (1982).
 - ²³ W. Janke and T. Sauer, *J. Chem. Phys.* **107**, 5821 (1997).
 - ²⁴ L. Brualla, K. Sakkos, J. Boronat, and J. Casulleras, *J. Chem. Phys.* **121**, 636 (2004).
 - ²⁵ M. Sprik, M. L. Klein, and D. Chandler, *Phys. Rev. B* **31**, 4234 (1985); *ibid.* **32**, 545 (1985).
 - ²⁶ M. E. Tuckerman, B. J. Berne, G. J. Martyna, and M. L. Klein, *J. Chem. Phys.* **99**, 2796 (1993).
 - ²⁷ S. R. Scuro and S. A. Chin, *Phys. Rev. E* **71**, 056703 (2005).
 - ²⁸ C. Chakravarty, M. C. Gordillo, and D. M. Ceperley, *J. Chem. Phys.* **109**, 2123 (1998).
 - ²⁹ C. Predescu, D. Sabo, J. D. Doll, and D. L. Freeman, *J. Chem. Phys.* **119**, 10475 (2003).
 - ³⁰ T. M. Yamamoto, *J. Chem. Phys.* **123**, 104101 (2005).
 - ³¹ R. A. Aziz, F. R. W. McCourt, and C. C. K. Wong, *Mol. Phys.* **61**, 1487 (1997).